Synthesis, characterization, and superoxide dismutase activity of two new copper(II) complexes of benzoylpyridine 4-phenylsemicarbazone

Ram N. Patel[a]

[a] Department of Chemistry, A.P.S. University, Rewa 486003, Madhya Pradesh, India

PLEASE SCROLL DOWN FOR ARTICLE

Taylor & Francis
Taylor & Francis Group

Synthesis, characterization, and superoxide dismutase activity of two new copper(II) complexes of benzoylpyridine 4-phenylsemicarbazone

RAM N. PATEL*

Department of Chemistry, A.P.S. University, Rewa 486003,
Madhya Pradesh, India

Two mononuclear complexes containing copper(II) and 2-benzoylpyridine 4-phenylsemicarbazone (BPS) and pseudohalides, $[Cu(BPS)(N_3)]$ (**1**) and $[Cu(BPS)(NCS)(H_2O)]NO_3$ (**2**) have been synthesized and characterized by UV-Vis, Fast atom bombardment, electron paramagnetic resonance, and infrared spectroscopy. Crystal structures of these two complexes have been resolved by using single crystal X-ray studies. Complex **1** crystallizes in the triclinic lattice with space group *P1* and is a distorted square planar geometry. Complex **2** also crystallizes in the triclinic lattice with space group *P1* but is a distorted square pyramidal geometry with N_3O_2 chromophore. Both the complexes have $g_\parallel > g_\perp > 2.0023$ and a *G* value less than 4, consistent with a $d_{x^2-y^2}$ ground state. Superoxide dismutase activities have also been examined.

Keywords: Copper(II) complexes; Super oxide dismutase (SOD); Pseudohalides; Crystal structure

1. Introduction

Pseudohalides with versatile coordination modes to monomeric, dimeric, and polymeric complexes [1–9] exhibit super exchange pathway for propagating magnetic interactions between paramagnetic centers. Copper complexes of azides and thiocyanates are of considerable interest mainly due to coordination geometry, molecular structures, and spectroscopic properties as well as biochemical importance [10–12].

Mixed ligand complexes play important roles in biological processes as exemplified by many enzymes activated by metal ions [13, 14]. Copper(II) complexes have found possible medical uses in the treatment of many diseases, including cancer [15, 16]. Also, the synthesis of low molecular weight copper(II) complexes with super oxide dismutase (SOD) activity has been challenging for bioinorganic chemists and for many years efforts have been made to obtain complexes with high catalytic activity [17–35]. Copper(II) mononuclear complexes, especially analogues of binuclear copper(II) complexes that mimic the activities of metalloproteins, may be considered as models

*Email: rnp64@yahoo.co.uk

for metalloproteins. Benzoylpyridine 4-phenylsemicarbazone (BPS) is a tridentate ligand with donor groups forming two five-membered chelate rings. A series of Schiff bases and their metal complexes have similar activity to the SOD enzyme [36, 37], but the relationship between structure and function has rarely been explored. In this article, structures for [Cu(BPS)(N$_3$)] (**1**) and [Cu(BPS)(NCS)(H$_2$O)]NO$_3$ (**2**) along with the spectroscopic and redox properties of the complexes are presented; SOD activity of these complexes have also been studied.

2. Experimental

2.1. *Materials*

Copper(II) nitrate trihydrate, sodium azide, and ammonium thiocyanate were purchased from S.D. Fine Chemicals, India. All other chemicals were of synthetic grade and used as received.

2.2. *Physical measurements*

2.2.1. Fast atomic bombardment mass spectra.   These spectra (Fast atomic bombardment; FAB) were recorded on a JEOL SX 102/DA 6000 Mass Spectrometer using xenon (6 kV, 10 mA) as the FAB gas. The accelerating voltage was 10 kV and the spectra were recorded at room temperature (RT) with *m*-nitrobenzoyl alcohol as the matrix.

2.2.2. Magnetic measurements.   Room temperature magnetic susceptibilities were measured by a Gouy balance using a mercury(II) tetrathiocyanato cobaltate(II) as calibrating agent ($\chi_g = 16.44 \times 10^{-6}$ cgs units). Diamagnetic corrections were estimated from Pascal's tables.

2.2.3. Spectrometry.   The ligand field spectra were recorded at 25°C on a Shimadzu UV-Vis recording spectrophotometer UV-1601 in solution. IR-spectra were recorded in KBr on a Perkin Elmer 783 spectrophotometer. X-band electron paramagnetic resonance (EPR) spectra were recorded on a Varian E-line Century Series Spectrometer equipped with a dual cavity and operating at X-band with 100 kHz modulation frequency. Tetracyanoethylene (TCNE) was used as field marker.

2.2.4. Electrochemistry.   Cyclic voltammetry (CV) was carried out with a BAS-100 Epsilon electrochemical analyzer having an electrochemical cell with a three-electrode system. Ag/AgCl was used as a reference electrode, glassy carbon as working electrode, and platinum wire as an auxiliary electrode; 0.1 M NaClO$_4$ was used as supporting electrolyte and DMSO as solvent. All measurements were carried out at 298 K under a nitrogen atmosphere.

2.2.5. SOD activity. The *in vitro* SOD activity was measured using alkaline DMSO as a source of superoxide radical (O_2^-) and nitrobluetetrazolium chloride (NBT) as O_2^- scavenger [38, 39]. In general, 400 µL sample to be assayed was added to a solution containing 2.1 mL of 0.2 mol potassium phosphate buffer (pH 8.6) and 1 mL of 56 µmol alkaline DMSO solution was added while stirring. The absorbance was then monitored at 540 nm against a sample prepared under similar condition except that NaOH was absent in DMSO. A unit of SOD activity is the concentration of complex, which causes 50% inhibition of the alkaline DMSO-mediated reduction of NBT.

2.3. *Synthesis*

2.3.1. Ligand (HL). HL was synthesized by refluxing 2-benzoylpyridine (1.832 g, 10 mmol) and 4-phenylsemicarbazide (1.512 g, 10 mmol) in ethanol for 1 h. The crystals appeared immediately after cooling to room temperature (yield, 70–80%). Anal. Calcd (%): C, 72.00; H, 5.06; N, 17.70. Found (%): C, 72.06; H, 5.01; N, 17.73.

2.3.2. Synthesis of [Cu(BPS)(N$_3$)] (1). A solution of $Cu(ClO_4)_2 \cdot 6H_2O$ (0.740 g, 2.0 mmol), BPS (0.620 g, 2.0 mmol), and NaN_3 (0.13 g, 2.0 mmol) were mixed in methanol (MeOH) and stirred well. After 30 min, the green solution was filtered and the supernatant liquid was kept in air for slow evaporation. Light green crystals of [Cu(BPS)N$_3$] were collected, washed with ether, and dried in a $CaCl_2$ desiccator (yield 65%). Anal. Calcd (%): C, 54.17; H, 3.56; N, 23.28. Found (%): C, 54.18; H, 3.55; N, 23.29.

2.3.3. Synthesis of [Cu(BPS)(NCS)(H$_2$O)]NO$_3$ (2). To a MeOH solution (10 mL) of copper(II) nitrate trihydrate (0.24 g, 1 mmol), a MeOH solution (10 mL) of benzoylpyridine (0.390 g, 1 mmol) was added with stirring for 10 min. To this mixture, a MeOH solution (10 mL) of ammonium thiocyanate (0.076 g, 1 mmol) was added and stirring was continued for 30 min at 25°C. The green solution was filtered to remove any solid impurities and left for slow evaporation. Green crystals of [Cu(BPS)(NCS)(H$_2$O)]NO$_3$ thus formed were collected, washed with ether, dried in air at room temperature, and stored in a $CaCl_2$ desiccator (yield 70%). Anal. Calcd (%): C, 46.33; H, 3.47; N, 16.2; S, 6.78. Found (%): C, 46.37; H, 3.49; N, 16.21; S, 6.80.

2.3.4. Crystal structure determination. Crystals suitable for X-ray analysis for **1** and **2** were grown from the slow evaporation of the reaction mixtures at room temperature. Single crystals suitable for X-ray study were mounted on a glass fiber and used for data collection. Crystal data were collected on an Enraf-Nonius MACH$_3$ diffractometer using graphite monochromated Mo-Kα radiation ($\lambda = 0.71073$ Å). The crystal orientation, cell refinement, and intensity measurements were made using CAD-4PC performing Ψ-scan measurements. The structures were solved by direct methods using SHELXS-97 [40] and refined by full-matrix least-square techniques against F^2 using SHELXL-97 [41]. All non-hydrogen atoms were refined anisotropically. All hydrogens were placed at calculated position and allowed to refine using a riding model.

3. Results and discussion

Copper(II), BPS, and pseudohalides form complexes with microanalysis consistent with its proposed stoichiometry. The molar conductance of **1** in 10^{-3} M DMF solution is $17 \, \text{ohm}^{-1} \, \text{cm}^2 \, \text{mol}^{-1}$, showing that this is a nonconductor [42]. The molar conductance of **2** is $80 \, \text{ohm}^{-1} \, \text{cm}^2 \, \text{mol}^{-1}$, consistent with 1:1 electrolyte as suggested by formula.

3.1. *Magnetic moments*

The magnetic measurements were carried out on the same samples that were analyzed structurally. The room temperature magnetic moments (1.83 B.M. for **1** and 1.85 B.M. for **2**) are close to the value expected for uncoupled copper(II) system and suggest the absence of spin exchange [36, 37, 43].

3.2. *Crystal structure of [Cu(BPS)(N₃)] (1) and [Cu(BPS)(NCS)(H₂O)]NO₃ (2)*

The thermal ellipsoid drawings of the two molecular structures with atom numbering schemes are shown in figures 1 and 2. The crystallographic data are given in table 1 and selected bond lengths and angles are given in tables 2 and 3.

Complex **1** crystallizes with two monomers per asymmetric unit in the triclinic crystal system. The crystal structure contains two crystallographically independent but chemically equivalent [Cu(BPS)(N₃)] molecules tied in an infinite 3-D network by hydrogen-bonding interactions; a drawing of the unit cell contents is shown in figure 3.
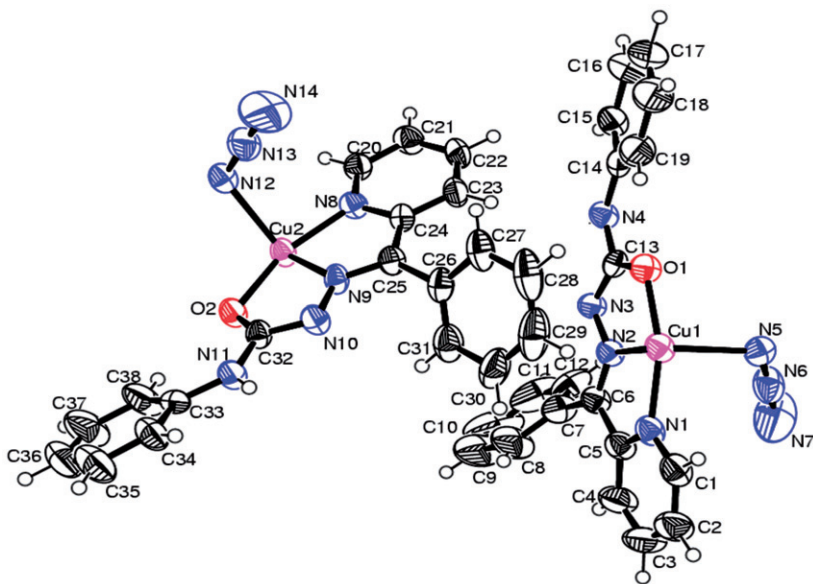

Figure 1. Projection view of **1**.
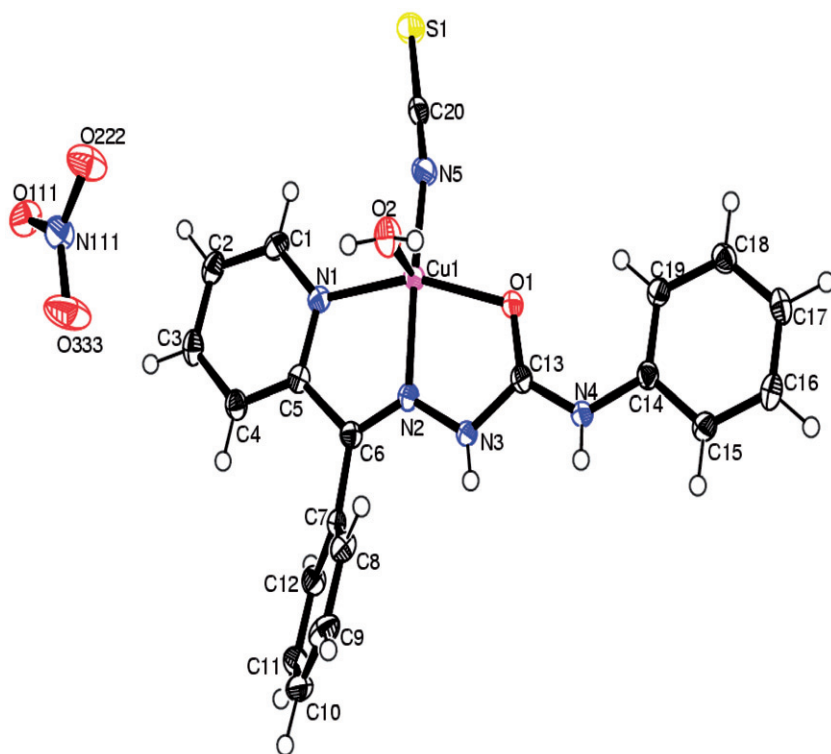
Figure 2. Projection view of **2**.

Table 1. Crystal data and structure refinement parameters for **1** and **2**.

Empirical formula	$C_{38}H_{30}Cu_2N_{14}O_2$	$C_{20}H_{18}CuN_6O_5S$
Formula weight	841.84	518.00
Temperature (K)	150(2)	150(2)
Wavelength (Å)	0.71073	0.71073
Crystal system	Triclinic	Triclinic
Space group	*P 2(1)/c*	*P 2(1)/c*
Unit cell dimensions (Å, °)		
a	8.1264(5)	9.8108(5)
b	11.0060(11)	10.8777
c	21.6375(16)	10.9755(6)
α	75.463(8)	92.317(4)
β	84.253(6)	101.578(5)
γ	83.926(7)	108.343(4)
Volume (Å^3), *Z*	1857.3(3), 2	1082.38(9), 2
Calculated density (mg cm^{-3})	1.505	1.589
F(000)	860	530
Crystal size (mm^3)	$0.33 \times 0.27 \times 0.22$	$0.23 \times 0.17 \times 0.15$
θ range for data collection (°)	2.99–25.00	3.26–24.99
Reflections collected	14,004	9487
Parameters	513	314
Goodness-of-fit on F^2	0.970	1.097
Final *R* indices [$I > 2\sigma(I)$]	$R_1 = 0.0555$, $wR_2 = 0.0763$	$R_1 = 0.0237$, $wR_2 = 0.0645$
Largest difference peak and hole (e Å^{-3})	0.277 and −0.299	0.305 and −0.275

Table 2.   Selected bond lengths (Å) and angles (°) of **1**.

Cu(1)–N(5)	1.9043(16)	Cu(1)–N(1)	2.0027(15)
Cu(1)–N(2)	1.9479(15)	Cu(1)–O(1)	2.0242(13)
N(5)–Cu(1)–N(2)	167.8(7)	N(5)–Cu(1)–O(1)	99.5(6)
N(5)–Cu(1)–N(1)	99.6(6)	N(2)–Cu(1)–O(1)	79.0(5)
N(2)–Cu(1)–N(1)	79.7(6)	N(1)–Cu(1)–O(1)	157.3(6)

Table 3.   Selected bond lengths (Å) and angles (°) of **2**.

Cu(1)–N(2)	1.937(3)	Cu(1)–N(1)	2.000(3)
Cu(1)–O(1)	1.953(3)	Cu(1)–N(5)	2.403(4)
Cu(1)–N(5)	1.957(3)		
N(2)–Cu(1)–O(1)	80.2(1)	O(1)–Cu(1)–O(2)	96.1(6)
N(1)–Cu(1)–O(2)	92.9(6)	N(2)–Cu(1)–O(2)	93.4(6)
N(5)–Cu(1)–O(2)	98.7(6)	O(1)–Cu(1)–N(1)	160.0(1)
N(2)–Cu(1)–N(1)	80.6(1)	N(2)–Cu(1)–N(5)	102.3(1)
N(1)–Cu(1)–N(5)	92.8(1)	O(1)–Cu(1)–N(5)	96.7(1)
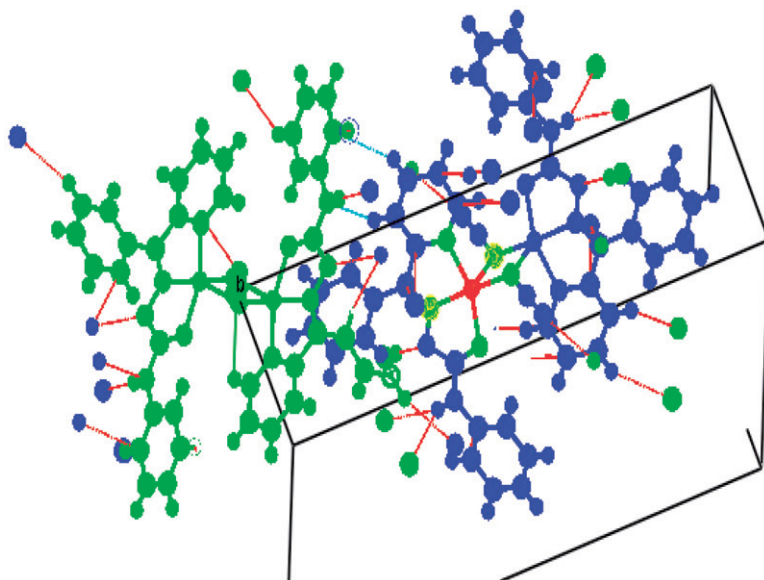
Figure 3.   Structure showing the arrangement of **1**.

The network of intra- and intermolecular hydrogen bond interactions on which the crystal packing depends is presented in table 4. Two intermolecular H-bond interactions, N(4)–H(4)–N(11) and N(11)–H(11)–N(3), and four intramolecular H-bond interactions, C(19)–H(19)–O(1), C(20)–H(20)–O(2), C(31)–H(31)–N(10), and C(38)–H(38)–O(2), exist. Copper is a distorted square planar geometry with donors being pyridine nitrogen N(1), imine nitrogen N(2), and O(1) from the tridentate benzoylpyridine semicarbazonato ligand and N(5) from azide. Binding parameters agree with the coordination of BPS in the enolate form. The complex deviates

Table 4. Hydrogen bonding interactions for **1**.

D–H⋯A	D–H (Å)	H⋯A (Å)	D⋯A (Å)	∠D–H⋯A (°)
N(4)–H(4N) ⋯N(10)[a]	0.88(3)	2.09(3)	2.969(5)	175(3)
N(11)–H(11N) ⋯N(3)[a]	0.81(3)	2.39(3)	3.185(5)	166(3)

Symmetry transformations used to generate equivalent atoms: [a]$-x$, $1-y$, $1-z$.

considerably from the square planar geometry. The dihedral angle between mean planes of chelate rings is 53.89(0.13)°. The difference between the internal geometries of two independent BPS ions occurs at five-membered chelate rings with the torsion angles at the C–C bonds of 3.08(0.14)° and 4.92(0.15)°, respectively. These values are in the range 0–30° observed for other similar mononuclear complexes having five-membered rings [44, 45]. Similar mononuclear complexes [46, 47] containing pseudohalides were also characterized. The geometry around copper(II) has tetrahedral distortion, evident from the value of the *transoid* angles N(1)–Cu(5)–O(1) = 157.3(6)°, and N(2)–Cu(1)–N(5) = 167.8(7)°. Comparing this complex with a similar complex in which the N(4) substituent is cyclohexyl [48], there exists appreciable variation in C(13)–N(4) bond length (1.344(5) Å), compared to the value of 1.339(3) in the complex containing N(4) substituent as cyclohexyl. This is due to the delocalization of the lone pair of electrons of N(4) with the phenyl ring [47]. The bond angle N(6)–N(5)–Cu(1) 117.8(3) Å reveals that the Cu–N–N coordination is nonlinear, while the linearity of N(5)–N(6)–N(7) 178.5(5)° is retained.

Complex **2** crystallizes as blue-green single crystals in triclinic system with a space group *P1*. The copper(II) is coordinated by two nitrogens and one oxygen of BPS, one nitrogen of thiocyanate and one oxygen of water in a square pyramid (SP). The complex cation is neutralized by NO_3^-, thus proving the coordination of BPS *via* the ketone form. The basal plane of the SP consists of N(1), N(2), O(1), and N(3), where N(2) is *trans* to N(5) of NCS. O(2) is apically coordinated at 2.2237(15) Å, greater than Cu–O(1) distance (2.0241(13) Å). Longer Cu-axial ligand bonds are frequently observed in copper(II) complexes. Copper–nitrogen distances Cu(1)–N(5) 1.9043(18), Cu(1)–N(2) 1.9479(15), and Cu(1)–N(1) 2.0027(05) Å are almost equal and consistent with distances usually found for SP [49] copper(II) with nitrogen ligands.

The angles around copper in the basal plane N(2)–Cu(1)–N(1) 79.70(6)°, N(2)–Cu(1)–O(1) 79.04(5)° and the angles N(5)–Cu(1)–O(1) 99.48(6)° and N(5)–Cu(1)–N(1) 99.64(6)° are in the expected range. Angles with O(2) remain in the range 92.9(6)–98.73(6)°, proving the distortion of the basal plane. The *trans* bond angles deviate from 180°: N(1)–Cu(1)–O(1) 157.3(6) and N(3)–Cu(1)–N(2) 167.8(7) further confirming the distortion of the SP. Two five-membered chelate rings have a distorted envelope conformation with different values of deviation (0.0240 and 0.0407 Å) of the copper(II) ion from the mean plane defined by the four other atoms forming the chelate rings. The degree of distortion in the five-coordinate complex may be quantified by the geometrical factor (τ) that represents the degree of trigonal bipyramid (TBP) distortion from the ideal SP geometry ($\tau = 0$ for ideal SP and 100% for ideal TBP) [50, 51]. The ratio between the two basal angles that would form the basal plane in the SP structure defines $\tau = [(\theta - \phi)/60] \times 100$. For this complex, $\theta = 167.85(7)°$ and $\phi = 157.34(6)°$, yields ≈18%, indicating significant distortion from the ideal SP in the

solid state. Significant H-bond interactions are seen and H-bonding data are given in table 5. Perspective view of the crystal packing in a unit cell is shown in figure 4.

3.3. *EPR spectra*

X-band EPR spectra of polycrystalline complexes at RT and in DMSO at liquid nitrogen temperature (LNT) were recorded using 100 KHz field modulation; *g* factors are quoted relative to the standard field marker TCNE ($g_e = 2.00277$). The EPR spectral parameters of the copper(II) complexes along with the spin Hamiltonian and orbital

Table 5. Hydrogen bonding interactions for **2** (Å and °).

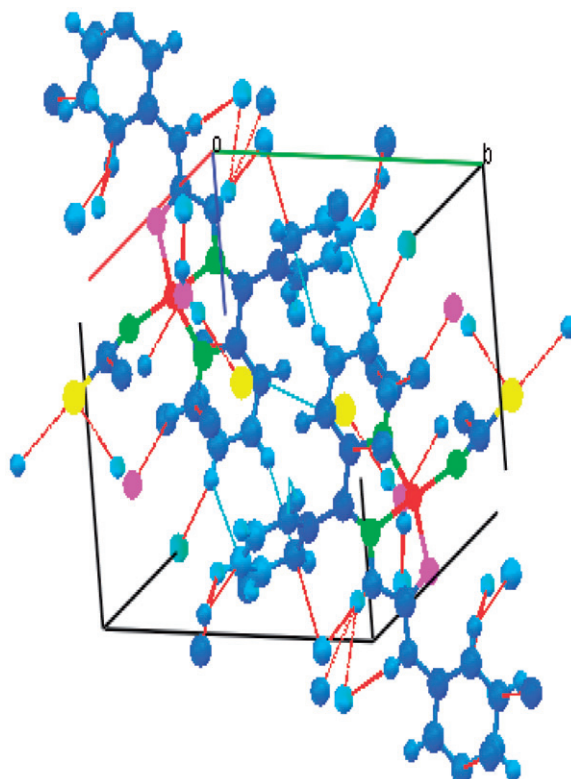| D–H···A	D–H (Å)	H···A (Å)	D···A (Å)	∠D–H···A (°)
N(3)–H(3N)···O(111)	0.75(2)	2.05(2)	2.784(2)	167(3)
N(4)–H(4N)···O(222)	0.77(2)	2.06(2)	2.819(2)	167(2)
O(2)–H(101)···O(222)	0.81(3)	1.93(3)	2.730(2)	174(3)
O(2)–H(102)···S(1)	0.81(2)	2.54(2)	3.3417(18)	170(3)
C(1)–H(1)···O(2)	0.95	2.53	3.356(3)	145
C(2)–H(2)···O(333)	0.95	2.51	3.314(3)	143
C(12)–H(12)···O(111)	0.95	2.39	3.213(3)	145

Figure 4.   Structure showing the arrangement of **2**.

reduction parameters are given in table 6. The EPR spectra of the complexes polycrystalline state at RT in frozen solution (100% DMSO at LNT) are provided in the "Supplementary material".

At RT, the complexes show axial symmetry $g_2 \geq g_1$ with well-defined $g_\parallel$ (g_3) and $g_\perp$ ($(g_1 + g_2)/2$) values. The geometric parameter G, which is a measure of the exchange interaction between the copper center in the polycrystalline complex, is calculated by using [52]: $G = g_\parallel - 2.0023/g_\perp - 2.0023$ for an axial spectrum. Both complexes with $g_\parallel > g_\perp > 2.0023$ and G values less than 4.0 are consistent with a $d_{x^2 - y^2}$ ground state in a square planar or SP geometry [53, 54].

The frozen solution X-band EPR spectra show axial character with $g_\parallel > g_\perp = 2.0023$ [55, 56]. The value of $g_\parallel < 2.3$ suggests the covalent nature of both complexes and the presence of mixed copper–nitrogen and copper–oxygen bonds. The in-plane σ- and π-bonding are related to the α and β parameters, respectively (table 6). In addition, γ values are representative of out-of-plane π-bonding. The value of the in-plane σ-bonding parameter α^2 was calculated using [57]: $\alpha = (A_\parallel/(0.036) + (g_\parallel - 2.0023) + 3/7 (g_\perp - 2.0023) + 0.036$ for copper(II) complexes with $^2B_{1g}$ ground state ($g_\parallel > g_\perp$), the g values may be expressed as follows:

$$K_\parallel^2 = (g_\parallel - 2.0023)E_{d-d}/8\lambda_0$$

$$K_\perp^2 = (g_\perp - 2.0023)E_{d-d}/2\lambda_0$$

where λ_0 is the spin-orbit coupling constant, with a value of $-828\,\mathrm{cm}^{-1}$ for a copper(II) d^9 system. $K_\parallel$ and $K_\perp$ are the parallel and perpendicular reduction components of the orbital reduction factor (K). The calculated values of $K_\parallel$ and $K_\perp$ for present complexes are close to those reported for similar complexes for pure σ-bonding, $K_\parallel \approx K_\perp \approx 0.77$ and for in-plane π-bonding $K_\parallel < K_\perp$, while for out-of-plane π-bonding, $K_\parallel > K_\perp$ [53]. For [Cu(BPS)(NCS)(H$_2$O)]NO$_3$ $K_\parallel > K_\perp$, indicating significant out-of-plane π-bonding, [Cu(HL)N$_3$] $K_\parallel < K_\perp$ indicates significant in-plane π-bonding.

Table 6. The EPR spectral parameters of the copper(II) complexes.

	1	2
Polycrystalline state (RT)		
$g_\parallel$ (g_3)		2.261
$g_\perp$ ($(g_1 + g_2)/2$)		2.066
G		3.95
Frozen solution (LNT)		
$g_\parallel$	2.210	2.268
$g_\perp$	2.056	2.073
$A_\parallel$ (G)	165	150
G	3.867	3.758
α^2	0.6555	0.7208
β^2	1.0526	1.0682
γ^2	1.0373	1.0821
$K_\parallel$	0.69	0.77
$K_\perp$	0.68	0.78
f (cm)	143	–

The estimated values of α^2, β^2, and γ^2 of the complexes are consistent with the strong in-plane σ- and out-of-plane π-bonding for $[Cu(BPS)(NCS)H_2O]NO_3$ and in-plane π-bonding for $[Cu(BPS)(N_3)]$. The distortion from the plane increases with increasing g value and decreasing A_{11} values. So the value of $g_{\parallel}/A_{\parallel}$ ratios (empirical factor, f) is a good criterion to determine the distortion level [58]. The f is an index of tetragonal distortion and may vary from 105 cm to 135 cm for small to extreme distortions in square planar complexes [58]. The f value for $[Cu(BPS)(N_3)]$ is 143 cm, indicating significant distortion from planarity.

3.4. *Infrared spectral study*

In infrared spectra, the point of interest is the band due to azide and thiocyanate in the complexes. The IR spectrum of $[Cu(BPS)(N_3)]$ has a very strong and sharp absorption at 2055 cm^{-1} due to the asymmetric stretching [59] of the terminal azide, close to those observed in azido monomeric copper(II) complexes [60–62]. $[Cu(BPS)(NCS)H_2O]$ shows a characteristic strong transmission at 2100 cm^{-1} along with a weak band at 2095 cm^{-1} which corresponds to NCS$^-$ [63, 64]. A strong broad absorption for **2** at 3456 cm^{-1} is associated with the coordinated water molecule. A sharp, single nitrate combination ($\gamma_1 + \gamma_4$) band [65] at 1767 cm^{-1} indicates the presence of ionic nitrate.

The $\gamma(C=N)$ of the ligand at 1623 cm^{-1} shifts to 1565–1597 cm^{-1} in the complexes, indicating the coordination *via* azomethine nitrogen. One IR band at $\sim$990 cm^{-1} associated with a pyridine ring breathing mode [66] shifts to higher energies on coordination, occurring at 995 cm^{-1} in **1** and 1005 cm^{-1} in **2**. The $\gamma(M–O)$ appears in complexes at 430–487 cm^{-1}.

3.5. *Ligand field spectra*

The ligand field spectra (Supplementary material) for both complexes were recorded in DMSO. The spectrum of **1** exhibits a strong band at 415 nm assigned to a ligand-to-metal charge transfer absorption, typical of Cu-L complexes [67]. The weaker d–d band at 700 nm is consistent with a distorted SP geometry similar to that found in $[CuL(Sacc)(H_2O)]0.5H_2O$ (HL = 2-formyl pyridine thiosemicarbazone; HSacc = Saccharin) [68]. Similarly, $[Cu(BPS)(N_3)]$ exhibits two absorption bands, at 700 nm assigned to $^2B_{1g} \rightarrow {}^2B_{2g}$ and at 422 nm to $^2B_{1g} \rightarrow {}^2E_g$ transition. These absorptions correspond to a distorted square-planar environment around copper(II) [69].

3.6. *Electrochemistry*

The cyclic voltammogram (CV) of **1** exhibits a single irreversible wave at -585 mV (scan rate 100 mV s^{-1}) and -550 mV (scan rate 200 mV s^{-1}), which can be attributed to the Cu$^{II} \rightarrow$ Cu^{I} redox process [70, 71] (table 7). The CV of **2** shows a sharp oxidation peak during the reverse scan, which is tentatively attributed to adsorption of the complex onto the electrode surface. Alternatively, the deposit of reduced copper species on the electrode surface may give rise to the typical features of a redissociation process during the reverse scan [71]. Scans are provided in the "Supplementary material".

Table 7.   CV data for 1 mmol solution of the Cu(II) complexes in DMSO containing 0.1 M $NaClO_4$ as supporting electrolytes.

Scan rate ($mV s^{-1}$)	E_{pc} (mV)	I_{pc} (μA)	E_{pa} (mV)	I_{pa} (μA)	ΔE_p (mV)	E° (mV)
$[Cu(BPS)(N_3)]$						
100	−585	0.9823	−260	1.0356	325	423
200	−550	1.6754	−294	2.2248	256	422
$[Cu(BPS)(NCS)(H_2O)]NO_3$						
100	−594	05728	250	5.0752	844	422
200	−548	1.8372	294	3.5920	842	421

$\Delta E_p = E_{pa} - E_{pc}$; $E^\circ = (E_{pa} + E_{pc})/2$.

Table 8.   SOD activity of some copper(II) complexes.

Complex	IC_{50} ($\mu mol\, dm^{-3}$)	References
$[Cu(glygly)] \cdot 3H_2O$	132	[39]
$[Cu(SAA)(Phen)]$	50	[36]
$[Cu(SAA)(Me\, ImH)]$	35	[37]
$[Zn(salgly)(phen)H_2O]$	6.15	[37]
$[Cu(salgly)(phen)H_2O]$	0.79	[37]
$[Cu(BPS)(N_3)]$	29	This work
$[Cu(BPS)(CNS)(H_2O)]NO_3$	11	This work

3.7. *Superoxide dismutase activity*

Superoxide dismutase activity of both the complexes is presented in table 8 along with the activity data of similar mononuclear complexes [36, 37, 39]. The data suggest that the distorted geometry of these complexes favors the geometrical change essential for catalysis as the geometry of copper in the SOD enzyme also changes into distorted SP [37, 39] geometry. The data suggest that **1** with square planar geometry shows moderate activity, while **2** shows higher activity. An interaction between super oxide ion and Cu(II) is induced due to the stronger axial bond present in **2**, which results in increased catalytic activity [72].

4. Conclusion

In summary, $[Cu(BPS)(N_3)]$ and $[Cu(BPS)(NCS)(H_2O)]NO_3$ were synthesized and characterized by single crystal X-ray, CV, and spectroscopy (IR, UV-Vis, and EPR). Competition with NBT toward superoxide shows the same result for **1** and better for **2**, although the SOD activity for **2** is not higher than that of some reported complexes [36, 37, 39]. This study demonstrates that it is possible to enhance the SOD activity of copper(II) complexes with an appropriate modification in the coordination geometry. Complex **2** having similar geometry to that of native SOD may be considered an analogue.

Supplementary material

CCDC 704271 and 704270 contain the supplementary crystallographic data for [Cu(BPS)(N$_3$)], **1** and [Cu(BPS)(NCS)(H$_2$O)]NO$_3$, **2**, respectively. These data can be obtained free of charge *via* http://www.ccdc.cam.ac.uk/conts/retrieving.html or from the Cambridge Crystallographic Data Centre, 12 Union Road, Cambridge CB2 1EZ, UK; Fax: +44-1223-336033; or Email: deposit@ccdc.cam.ac.uk. Other supplementary data such as FAB mass spectra, etc., to readers may be available from author on request.

Acknowledgments

References

[1] P. Manikandan, R. Muthukumaran, K.R. Thomas, B. Varghese, G.V.R. Chandramouli, P.T. Manoharan. *Inorg. Chem.*, **40**, 2378 (2001).
[2] S. Dalai, P.S. Mukherjee, M.G.B. Drew, T.-H. Lu, N.R. Chaudhuri. *Inorg. Chim. Acta*, **355**, 85 (2002).
[3] A. Escuer, M.A.S. Goher, F.M. Mautner, R. Vicente. *Inorg. Chem.*, **39**, 2107 (2000).
[4] L. Li, D. Liao, Z. Jiang, S. Yan. *Polyhedron*, **20**, 681 (2001).
[5] T.K. Karmakar, S.K. Chandra, J. Ribas, G. Mostafa, T.H. Lu, B.K. Ghosh. *Chem. Commun.*, 2364 (2002).
[6] D. Bose, S.H. Rahaman, G. Mostafa, R.D. Bailey Walsh, M.J. Zaworotko, B.K. Ghosh. *Polyhedron*, **23**, 545 (2004).
[7] J. Banerjee, D. Bose, S.H. Rahaman, M.J. Zaworotko, B.K. Ghosh. *Indian J. Chem.*, **43A**, 1119 (2004).
[8] J.P. Costes, J. Ruiz, F. Dahan, J.P. Laurent. *Inorg. Chim. Acta*, **239**, 53 (1995).
[9] S.S. Massoud, F.A. Mautner. *Inorg. Chim. Acta*, **358**, 3334 (2005).
[10] S.H. Rahaman, D. Bose, R. Ghosh, H.-K. Fun, B.K. Ghosh. *Indian J. Chem.*, **43A**, 1901 (2004).
[11] G. Wilkinson. *Comprehensive Coordination Chemistry*, Vol. 5, p. 775, Pergamon Press, Oxford (1987).
[12] K.D. Karlin, J. Zubieta (Eds.). *Copper Coordination Chemistry*: *Biochemical and Inorganic Perspectives*, Adenine Press, Guilderland, New York (1983).
[13] L. Halleman, C.C. Stock. *J. Biol. Chem.*, **125**, 77 (1938).
[14] B.L. Valle, J.E. Coleman. *Compr. Biochem.*, **8**, 1458 (1968).
[15] J.R.J. Sorenson. *Chem. Br.*, **16**, 1110 (1984).
[16] R.K. Gouch, T.W. Kensler, L.W. Oberley, R.J. Sorenson. In *Biochemical and Inorganic Copper Chemistry*, K.D. Karlin, J. Zubieta (Eds), Vol. 1, p. 139, Adenine Press, New York (1986).
[17] K.G. Strotkamp, S.J. Lippard. *Acc. Chem. Res.*, **15**, 138 (1982).
[18] A. Gartner, U. Weser. *Top. Curr. Chem.*, **132**, 1 (1986).
[19] J.L. Pierre, P. Chautemps, S. Refaif, C. Beguin, A.E. Marzouki, G. Serratrice, E. Saint-Aman, P. Rey. *J. Am. Chem. Soc.*, **117**, 1965 (1995).
[20] U. Weser, L.M. Schubotz, E. Lengfelder. *J. Mol. Catal.*, **13**, 249 (1981).
[21] C.L. O'Young, J.C. Dewan, H.R. Lilienthal, S.L. Lippard. *J. Am. Chem. Soc.*, **100**, 7291 (1978).
[22] P.K. Caughlin, A.E. Martin, J.C. Dewan, E. Watanabe, J.E. Bulkoski, S.J. Lippard. *Inorg. Chem.*, **23**, 1004 (1984).
[23] P.K. Caughlin, S.J. Lippard. *Inorg. Chem.*, **23**, 1446 (1984).
[24] M.G.B. Drew, S.M. Nelson, J. Reedijk. *Inorg. Chim. Acta*, **64**, L189 (1982).
[25] M. Sato, M. Ikeda, J. Nakaya. *Inorg. Chim. Acta*, **93**, L61 (1984).
[26] J. Cabral, M.F. Cabral, M. McCann, S.M. Nelson. *Inorg. Chim. Acta*, **86**, L15 (1984).
[27] C.A. Salata, M.T. Youinou, C.J. Burrows. *J. Am. Chem. Soc.*, **111**, 9278 (1989).
[28] C.A. Salata, M.T. Youinou, C.J. Burrows. *Inorg. Chem.*, **30**, 3454 (1991).
[29] Q. Lu, Q.H. Luo, A.B. Dai, G.Z. Hu. *J. Chem. Soc., Chem. Commun.*, 1429 (1990).
[30] Z.W. Mao, K.B. Yu, D. Chen, S.Y. Han, Y.X. Sui, W.X. Tang. *Inorg. Chem.*, **32**, 3104 (1993).

[31] R.N. Patel, K.B. Pandeya. *J. Inorg. Biochem.*, **72**, 109 (1998).
[32] R.N. Patel, H.C. Pandey, K.B. Pandeya. *Synth. React. Inorg. Met.-Org. Chem.*, **10**, 1733 (1999).
[33] R.N. Patel, A.P. Patel, K.B. Pandeya. *Indian J. Chem.*, **38A**, 900 (1999).
[34] R.N. Patel, S. Kumar, K.B. Pandeya. *J. Inorg. Biochem.*, **72**, 109 (1998).
[35] R.N. Patel, S. Kumar, K.B. Pandeya. *Spectrochim. Acta, Sect. A*, **56**, 2791 (2000).
[36] R.N. Patel, V.L.N. Gundla, D.K. Patel. *Polyhedron*, **27**, 1054 (2008).
[37] J. Han, Y. Xing, C. Wang, P. Hou, F. Bai, X. Zeng, X. Zhang, M. Ge. *J. Coord. Chem.*, **62**, 745 (2009).
[38] R.N. Patel, N. Singh, K.K. Shukla, V.L.N. Gundla, U.K. Chouhan. *J. Inorg. Nucl. Chem.*, **89**, 651 (2005).
[39] R.G. Bhirud, T.S. Shrivastava. *Inorg. Chim. Acta*, **179**, 125 (1991).
[40] G.M. Sheldrick. *SHELXS, Program for the Solution for Crystal Structures*, University of Göttingen, Göttingen, Germany (1997); *Acta Crystallogr., Sect. A*, **46**, 467 (1990).
[41] G.M. Sheldrick. *SHELXL-97, Program for the Refinement of Crystal Structures*, University of Göttingen, Göttingen, Germany (1997).
[42] W.J. Geary. *Coord. Chem. Rev.*, **7**, 81 (1971).
[43] K. Skorta, S.P. Perlaps, C.P. Raptopoulou. *Transition Met. Chem.*, **24**, 541 (1999).
[44] H.C. Freeman. *Adv. Protein Chem.*, **22**, 257 (1967).
[45] L.A. Meiske, R.A. Jacobson, R.J. Angelici. *Inorg. Chem.*, **19**, 2034 (1980).
[46] M. Joseph, V. Suni, M.R.P. Kurup, M. Nethaji, A. Kishope, S.G. Bhat. *Polyhedron*, **23**, 3069 (2004).
[47] M. Joseph, M. Kuriakose, M.R.P. Kurup, M. Nethaji, A. Kishope, S.G. Bhat. *Polyhedron*, **23**, 3069 (2004).
[48] J.H. Liu, S.Y. Yang, C.Y. Duan, X.Z. You. *Chem. Lett.*, **10**, 1063 (1999).
[49] S.S. Massoud, F.A. Maunter. *Inorg. Chem. Commun.*, **7**, 559 (2004).
[50] A.W. Addison, T.N. Rao, J. Reedijk, J. vanRijn, G.C. Verchoor. *J. Chem. Soc., Dalton Trans.*, 1349 (1984).
[51] M. Duggan, N. Ray, B. Hathaway, G. Tomlinson, P. Brint, K. Pelin. *J. Chem. Soc., Dalton Trans.*, 1349 (1980).
[52] P.F. Rapheal, E. Manoj, M.R.P. Kurup. *Polyhedron*, **21**, 818 (2007).
[53] B.J. Hathaway, G. Willkinson, R.D. Gillard, J.A. McCleverty (Eds.). *Comprehensive Coordination Chemistry II*, Vol. 5, Pergamon Press, Oxford (1987).
[54] V. Philip, V. Suni, M.R.P. Kurup, M. Nethaji. *Polyhedron*, **24**, 1123 (2005).
[55] A. Garcia-Raso, J.J. Kiol, B. Adrover, P. Tauler, A. Pons, I. Mata, E. Espinesa, E. Motins. *Polyhedron*, **22**, 3255 (2003).
[56] J.Q. Klinman. *Chem. Rev.*, **96**, 2541 (1996).
[57] R. Klement, F. Stock, H. Elias, H. Paulus, P. Pelikan, M. Vollco, M. Mazur. *Polyhedron*, **18**, 3617 (1999).
[58] R. Pogni, M.C. Bartoo, A. Diaz, R. Basali. *J. Inorg. Biochem.*, **79**, 333 (2008).
[59] K. Nakamoto. *Infrared and Raman Spectra of Inorganic and Organic Chemistry Compounds*, p. 290, Wiley, New York (1986).
[60] N.K. Karan, S. Mitra, T. Motsushila, V. Gramlich, G. Rosair. *Inorg. Chim. Acta*, **332**, 87 (2002).
[61] U. Mukhopadhayay, I. Bernal, S.S. Massoud, F.A. Maunter. *Inorg. Chim. Acta*, **357**, 3673 (2004).
[62] S.S. Massod, F.A. Maunter, M. Abu-Youssef, N.M. Shuaib. *Polyhedron*, **18**, 2061 (1990).
[63] S.H. Rahaman, R. Ghosh, T.H. Lu, B.K. Ghosh. *Polyhedron*, **24**, 1525 (2005).
[64] D.X. West, G. Ertem, R.M. Makeever. *Transition Met. Chem.*, **10**, 41 (1986).
[65] A.B.P. Lever, E. Montovani, B.S. Ramaswamy. *Can. J. Chem.*, **49**, 1957 (1971).
[66] A.R. Tatritzky, A.R. Hands. *J. Chem. Soc.*, 2202 (1958).
[67] A.G. Bingham, H. Bogge, A. Muller, E.W. Ainscough, A.M. Brodie. *J. Chem. Soc., Dalton Trans.*, 493 (1987).
[68] E.W. Ainscough, E.W. Bakker, A.M. Brodie, R.J. Cresswell, J.D. Ranford, J.M. Waters. *Inorg. Chim. Acta*, **172**, 185 (1990).
[69] A.B.P. Lever. *Inorganic Electronic Spectroscopy*, 2nd Edn, Elsevier, Amsterdam (1997).
[70] M.C.B. de Oliveira, M. Scarpellini, A. Neves, H. Terenzi, A.J. Bortoluzzi, B. Szpoganics, A. Greatti, A.S. Mangrich, E.M. de Souza, P.M. Fernandez, M.R. Soares. *Inorg. Chem.*, **44**, 921 (2005).
[71] D. Zurita, C. Scheer, J.-L. Pierre, E. Saint-Amam. *J. Chem. Soc., Dalton Trans.*, 4331 (1996).
[72] J.P. Collman, T.R. Halbert, K.S. Suslick. In *Metal Ion Activation of Dioxygen*, T.G. Spiro (Ed.), p. 1, John Wiley, New York (1980).